

# Journal Pre-proof

A Novel Ex Vivo Tracheobronchomalacia Model for Airway Stent Testing and In Vivo Model Refinement

Abhijit Mondal, PhD, Gary A. Visner, DO, Aditya K. Kaza, MD, Pierre E. Dupont, PhD



PII: S0022-5223(23)00333-1

DOI: <https://doi.org/10.1016/j.jtcvs.2023.04.010>

Reference: YMTC 19013

To appear in: *The Journal of Thoracic and Cardiovascular Surgery*

Received Date: 25 January 2023

Revised Date: 14 March 2023

Accepted Date: 10 April 2023

Please cite this article as: Mondal A, Visner GA, Kaza AK, Dupont PE, A Novel Ex Vivo Tracheobronchomalacia Model for Airway Stent Testing and In Vivo Model Refinement, *The Journal of Thoracic and Cardiovascular Surgery* (2023), doi: <https://doi.org/10.1016/j.jtcvs.2023.04.010>.

This is a PDF file of an article that has undergone enhancements after acceptance, such as the addition of a cover page and metadata, and formatting for readability, but it is not yet the definitive version of record. This version will undergo additional copyediting, typesetting and review before it is published in its final form, but we are providing this version to give early visibility of the article. Please note that, during the production process, errors may be discovered which could affect the content, and all legal disclaimers that apply to the journal pertain.

Copyright © 2023 Published by Elsevier Inc. on behalf of The American Association for Thoracic Surgery

**TITLE:** A Novel Ex Vivo Tracheobronchomalacia Model for Airway Stent Testing and In Vivo Model Refinement

**AUTHORS:** Abhijit Mondal, PhD<sup>1,3</sup>, Gary A. Visner, DO<sup>2,4</sup>, Aditya K. Kaza, MD<sup>1,3,\*</sup>, Pierre E. Dupont, PhD<sup>1,3,\*</sup>

**AFFILIATIONS:** <sup>1</sup>Department of Cardiac Surgery, Boston Children's Hospital, Boston, MA

<sup>2</sup>Division of Pulmonary Medicine, Boston Children's Hospital, Boston, MA

<sup>3</sup>Department of Surgery, Harvard Medical School, Boston, MA

<sup>4</sup>Department of Pediatrics, Harvard Medical School, Boston, MA

\*Co-Senior Authors

**Funding:** This work was funded by the National Institutes of Health under grants R41HL158451 and R01HL135077.

**Conflicts of Interests:** P.E.D. and A.K.K are inventors on a U.S. patent application held by Boston Children's Hospital that covers helical stent technology.

**Corresponding Author:**

Abhijit Mondal, PhD.

Boston Children's Hospital

330 Longwood Avenue, Enders Building 306

Boston, Massachusetts 02115

Phone: 801-557-9844

24 Email: [abhijit.mondal@childrens.harvard.edu](mailto:abhijit.mondal@childrens.harvard.edu)

25 **Article word count:** 3497

Journal Pre-proof

**Keywords:** Tracheobronchomalacia, tracheomalacia, ex vivo model, airway stents, stent testing

**Abbreviations:**

25% Cartilage Resection (CR25), 50% Cartilage Resection (CR50), Cross-Sectional Area (CSA), Cartilage Single Incision (CSI), Control (CTR), Computed Tomography (CT), induced tracheobronchomalacia (iTBM), Pitch (P), Tracheobronchomalacia (TBM), Tracheomalacia (TM), Stent 1 (ST1), Stent 2 (ST2), Stent 3 (ST3), Wire Diameter (WD)

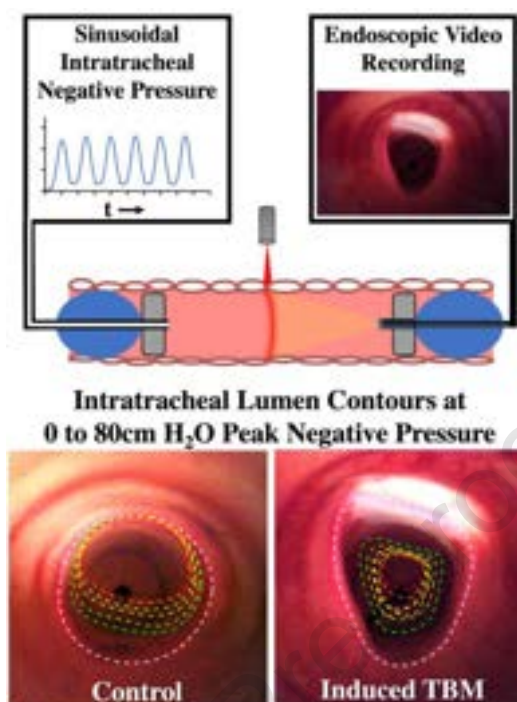
**Central Message:**

An ex vivo tracheal testing platform is described which enables the refinement of tracheobronchomalacia animal models and the rapid assessment of stent prototypes.

**Perspective Statement:**

We address the need for a physiologically accurate and inexpensive platform for rapid stent testing and design optimization. The presented platform provides video-based airway collapse measurement for pressure cycles corresponding to forced expiration in intact tracheas and malacic tracheas with and without helical stent support. The platform can also be used to refine malacic airway animal models.

44



45

46

47 **Central Picture.** Video tracking of ex vivo tracheal collapse for cyclic pressures of forced  
48 expiration.

**ABSTRACT**

**Objectives:** We sought to develop an ex vivo trachea model capable of producing mild, moderate and severe tracheobronchomalacia (TBM) for optimizing airway stent design. We also aimed to determine the amount of cartilage resection required for achieving different TBM grades that can be utilized in animal models.

**Methods:** We developed an ex vivo trachea test system which enabled video-based measurement of internal cross-sectional area as intratracheal pressure was cyclically varied for peak negative pressures of 20-80cm H<sub>2</sub>O. Fresh ovine tracheas were induced with TBM by single midanterior incision (n=4), midanterior circumferential cartilage resection of 25% (n=4) and 50% per cartilage ring (n=4) along a ~3cm length. Intact tracheas (n=4) were used as control. All experimental tracheas were mounted and experimentally evaluated. In addition, helical stents of two different pitches (6mm and 12mm) and wire diameters (0.52mm and 0.6mm) were tested in tracheas with 25% (n=3) and 50% (n=3) circumferentially resected cartilage rings. The percentage collapse in tracheal cross-sectional area was calculated from the recorded video contours for each experiment.

**Results:** Ex vivo tracheas compromised by single incision, 25% and 50% circumferential cartilage resection produce tracheal collapse corresponding to clinical grades of mild, moderate and severe TBM, respectively. A single anterior cartilage incision produces saber-sheath type TBM while 25% and 50% circumferential cartilage resection produce circumferential TBM. Stent testing enabled the selection of stent design parameters such that airway collapse associated with moderate and severe TBM could be reduced to conform to, but not exceed, that of intact tracheas (12mm pitch, 0.6mm wire diameter).

72 **Conclusion:** The ex vivo trachea model is a robust platform that enables systematic study and  
73 treatment of different grades and morphologies of airway collapse and TBM. It is a novel tool for  
74 optimization of stent design before advancing to in vivo animal models.

## INTRODUCTION

Tracheobronchomalacia (TBM) is the collapse of the large airway walls during expiration due to weakening of tracheal and mainstem bronchi segments in the supporting cartilage or the posterior membrane. When this weakening is limited only to the trachea, it is referred to as tracheomalacia (TM). Narrowing of the airway during expiration impedes airflow resulting in poor gas exchange. TBM is a progressive airway disease and while rare, it is observed in 13% of adults<sup>1</sup> and 30% of children<sup>2</sup> undergoing bronchoscopy. Symptoms leading to clinical presentation include dyspnea, episodic choking, chronic cough, hemoptysis and periodic respiratory infections.<sup>2</sup> TBM can be diagnosed and assessed using an awake functional bronchoscopy, dynamic computed tomography (CT) and pulmonary function studies.<sup>3</sup> The severity of the disease is graded based on the percentage reduction in the cross-sectional area (CSA) of the tracheal or bronchial lumen during forced expiration, deep breathing, Valsalva maneuver or coughing. For diagnosis and assessment dynamic bronchoscopy is considered the reference standard.<sup>4</sup> Dynamic CT provides a non-invasive option that enables quantitative assessment by mapping the extent of the disease over the entire tracheobronchial tree.<sup>5</sup> The disease is graded as mild, moderate or severe if the percentage reduction in CSA is between 51% to 75%, 76% to 90% or greater than 90%, respectively.<sup>4</sup> There is discussion on updating this scale range since studies have shown that even healthy patients have percentage collapse up to 70%.<sup>6</sup> TBM can be further classified based on the morphology of airway collapse corresponding to crescent, saber-sheath (or lateral) and circumferential.<sup>3</sup> Depending on the underlying disease, disease progression and severity, TBM can be treated by continuous positive airway pressure, stenting or surgery.<sup>3</sup>



Stenting is considered the preferred method of treating severe TBM in pediatric patients unable to manage with intermittent positive airway pressure ventilation.<sup>3</sup> In adults, severe TBM is treated surgically in carefully selected patients by tracheobronchoplasty or robotic tracheobronchoplasty.<sup>7</sup> In these patients stents also serve as an intermediate airway support before surgery. Several stenting options are available in a mesh or tube design made from silicone, nitinol, polyester, composites<sup>8</sup> and resorbable materials.<sup>9-12</sup> Complications associated with clinical use of silicone,<sup>13</sup> metal mesh<sup>14</sup> or resorbable<sup>10, 15, 16</sup> internal stents are well reported and require chronic airway management after implantation. Though no stent design is ideal, solid silicone tubes are the preferred clinical option. Recently, external resorbable stents<sup>9, 11</sup> show promise, but implantation requires complex surgery. Helical stents have generated some interest since they minimally affect mucus flow and provide the potential for atraumatic removal.<sup>17-20</sup> While most stents are designed as cylindrical tubes, non-circular profiles have also been developed that match the natural tracheal cross-sectional profile<sup>21</sup> to improve fitting and reduce stent migration.<sup>22, 23</sup>

Owing to the limitations and tradeoffs of existing devices, stent design continues to be an area of active research.<sup>8</sup> The design process is impeded, however, by limitations in the current mechanical testing methods and animal models available for refining and evaluating new stent concepts.

Initial design refinement is often performed using mechanical testing equipment to measure, e.g., a stent's radial and bending stiffness.<sup>24</sup> Since the literature suggests that stents of high stiffness are more prone to the generation of granulation tissue as well as to tissue erosion,<sup>8, 25</sup> these tests can be used to tune the design parameters of a new stent to match the stiffness of an existing stent that performs well with respect to these criteria.<sup>21, 24</sup> A challenge of this approach,

however, is that it is hard to understand how stiffness values relate to physiological conditions such as variation in airway CSA during specific breathing states. Furthermore, testing machines are typically designed for stents with circular cross sections bringing into doubt tests performed on non-circular stent profiles.

After initial refinement of a stent design, animal testing provides the most reliable platform for assessing both short- and long-term in vivo performance.<sup>26, 27</sup> In most animal models, TBM is surgically induced by partial or complete resection of tracheal cartilage rings while leaving intact the inner lumen of the trachea.<sup>26</sup> A significant challenge of these models is that the relationship between the fraction of cartilage removed and the grade of TBM is not known.

Ex vivo animal models represent an underutilized, but important middle ground between mechanical testing and animal models.<sup>21, 28, 29</sup> In this paper, we present an ex vivo testing system that enables initial stent designs of any cross-sectional profile to be rapidly and inexpensively compared in terms of airway cross-section under physiologic dynamic loading conditions. This testing system also helps to improve in vivo testing by providing a means to relate the amount of cartilage resected to clinical definitions of mild, moderate and severe TBM.

The system provides video-based measurement of tracheal cross-sectional area under cyclic pressure variations for peak negative pressures of 20-80cm H<sub>2</sub>O. This includes the intratracheal pressure range for TBM diagnosis by forced expiration.<sup>30</sup> In addition to determining the amount of cartilage resection corresponding to mild, moderate and severe TBM, we also relate the degree of resection to the morphology of collapse. To demonstrate how the system can be used for stent design, we show how the design parameters of a helical stent can be selected to reduce the collapse experienced with severe and moderate TBM to that of a healthy trachea.

## MATERIALS AND METHODS

### *Ex vivo testing system*

The testing system is depicted in the schematic of Figure 1A. The trachea is positioned over a warm water bath maintained at 37°C and is irrigated every 5-10 minutes with warm phosphate buffered saline. The tracheal lumen is sealed at both ends with latex balloons. The lumen of the balloon at the left end is connected to a pressure control circuit. The pressure circuit consists of a microprocessor-controlled (Arduino Uno, Bulk Construction Materials Initiative, Redmond, WA) linear actuator (Actuonix L12-EV3-100, Actuanix Motion Devices Inc, Victoria, BC, Canada) and pneumatic cylinder (Bore diameter: 1.5 inch, stroke: 4 inch, Parker Hannifin Corp., Mayfield Heights, OH) which is programmed to produce intratracheal negative pressure oscillations of a specified magnitude and frequency based on pressure sensor measurements (#159905, Radnoti LLC, Covina, CA). The actuator and cylinder were selected so that the model could produce oscillating intratracheal pressures with peak negative pressures of 20-80cm H<sub>2</sub>O and breathing rate of 20 breaths per minute. This fully covers the range reported for forced expiration as used in TBM diagnosis (average ~30cm H<sub>2</sub>O, maximum ~59cm H<sub>2</sub>O).<sup>30</sup>

The system was designed to apply oscillatory pressures for several reasons. First, initial testing demonstrated that tracheas maintained at static negative pressures sometimes remained collapsed after the negative pressure was removed. By applying an oscillating pressure, it was possible to compare the cross-sections between cycles to confirm that no permanent deformation had occurred. In addition, cyclic loading made it possible to perform tissue preconditioning by

running the system for an initial set of 6 cycles prior to data collection.<sup>31-33</sup> Finally, cyclic loading with a frequency matching the normal respiratory rate is more representative of physiologic conditions than static loading and provides information on the variation of the cross-section over a breathing cycle.

The microcontroller implements a feedback controller based on measured pressure to control actuator position and velocity. A safety reservoir is used to prevent any water from entering the cylinder or pressure transducer. Pressure commands are transferred from a PC by serial communication to the microcontroller and experimental data is collected on the PC using the same communication channel.

Two laser line generators (ELL1750 Laser Cube, Ryobi Ltd., Anderson, SC) are positioned on opposite sides of the trachea to create a closed contour on the tracheal cross-section whose area is to be measured (Figure 1A). The red laser light penetrates through the tracheal walls and is recorded to the PC using an endoscopic camera inserted through the lumen of the balloon at the right end. The experiments are performed without ambient light to maximize the contrast of the laser light.

### ***Ex vivo TBM model***

We procured fresh ovine tracheas (Research 89 Inc., Boston, MA) from the cervical region of similar intratracheal lumen diameter of 14mm-16mm for our study. All experiments were conducted within 36 hours of euthanasia and tissue harvest. The average cartilage width and inter-cartilage pitch of the study tracheas was measured.

Tracheas were prepared for four experimental conditions. The first condition served as control (CTR) with intact tracheas (1). The other 3 conditions presented three levels of induced

TBM (iTBM) by (2) single incision (CSI), (3) 25% radial cartilage resection (CR25) and (4) 50% radial cartilage resection (CR50) of ~3cm length. Each trachea was stretched and fixed in position on a tissue board using clamps. The region of the mid-anterior wall of the cartilage to be incised or transected was marked. For creating single incision condition, the center of the mid-anterior wall of the cartilage was incised without puncturing through the submucosal and transitional epithelial layers. For creating cartilage resection conditions, the selected portion of the cartilage were transected and carefully detached from the trachea while preserving the submucosal and transitional epithelial layers. Figure 2 shows representative tracheas for the four experimental conditions.

### ***Stent evaluation***

To demonstrate how the testing system could be used in stent design, three uncovered helical stent designs (Table 1) were evaluated in cyclic loading experiments. It has been shown that reduction of airway cross-section with this type of stent is comprised of two components.<sup>17,</sup><sup>19</sup> The first, which is typically the larger component, arises from the unsupported tissue between the coils bowing inward in a (helical) hourglass shape. The second component is due to radial compression of the helical coil. To assess the changes in airway reduction due to each of these components, the three stent designs listed below were tested. Stents 1 (ST1) and 2 (ST2) produce variation in the first component of collapse. They are made with the same wire diameter, but the pitch is doubled in Stent 2, which doubles the length of unsupported tissue between the coils. Stents 2 and 3 (ST3) produce variation in stent radial stiffness by using the same pitch, but different wire diameters.

### ***Cyclic loading experiments***

Each experimental trachea was mounted in the test system as described above. After fixing the trachea, tissue preconditioning was performed by applying 6 cycles at a magnitude of 20cm H<sub>2</sub>O. Subsequently, data was sequentially collected for 6 cycles per negative pressure magnitudes of (20,30,40,50,60,70,80) cm H<sub>2</sub>O using a period of 3s (blue curve in Figure 3D). Endoscopic video was recorded for each experiment and the videos were analyzed frame-by-frame to detect the laser-lit contour of the tracheal lumen (Figure 3E-F). This data was processed to compute reduction in CSA as a function of time and to determine the maximum reduction associated with the peak pressure.

Supplementary Table 1 list all the experimental conditions investigated using the test system in the order the experiments were performed. A total of 12 ovine tracheas were used. The control tracheas were also used for the single incision experiments. The tracheas with 25% and 50% cartilage resection were also used to test the three NiTi helical stents (Table 1) whose lengths were sufficient to cover the entire TBM region (Figure 1E).

### ***Data and statistical analysis***

A total of 238 endoscopic video clips corresponding to the 10 experimental conditions were recorded and analyzed. Automated tracheal lumen contour detection was performed frame-by-frame using MATLAB 2019 (Mathworks, Natick, MA). The process involved considering only the red channel of the color image. This was cropped from the side, contrast enhanced and filtered using a Gaussian filter (Figure 3C). The initial contour was set by detecting the peak pixel intensity along the radial direction from the center of the image. This was used as an initial guess for the Snake Contour method<sup>34, 35</sup> to detect the final intratracheal contour (Figure 3E and

3F). Video 1 shows the intratracheal contour and its calculated CSA in real-time for the experimental condition in Figure 3.

CSA of the closed contour is used to calculate the percentage collapse in the trachea at any given time,  $t$ :

$$\%collapse(t) = \frac{CSA(0) - CSA(t)}{CSA(0)} \times 100$$

For each experiment, the percentage collapse was plotted against time (Figure 3D) for all six cycles. The maxima were tabulated and the percentage collapse corresponding to the pressure value closest to the desired peak pressure value was selected.

To assess the significance of difference in percentage collapse between the experimental tracheas (CTR, CSI, CR25 and CR50), One-Way ANOVA tests (anova1.m, MATLAB 2019) were performed in MATLAB 2019. Student's t-tests (ttest2.m, MATLAB 2019) were performed pairwise for experimental conditions involving stents (ST1, ST2 and ST3). Statistical tests were performed separately for each pressure value. The maximum or minimum  $p$ -value has been reported to show significant or no significant difference, respectively.

## RESULTS

### *Severity of bronchomalacia versus amount of cartilage resected*

The average cartilage width of the tested tracheas was  $4.7\text{mm} \pm 1.0\text{mm}$  (range: 3.3mm-7.4mm). Resection of ~25% and ~50% corresponded to removing widths of  $15\text{mm} \pm 2\text{mm}$  (range: 13mm-19mm) and  $24\text{mm} \pm 2\text{mm}$  (range: 21mm-26mm), respectively. The average

center-to-center spacing between cartilage rings was  $6.5\text{mm} \pm 1.3\text{mm}$  (range: 4.8mm-8.8mm).  
The number of rings incised or resected was  $4.1 \pm 0.6$  (range: 3-5).

Figure 4 summarizes the results from the experiments conducted on intact and malacic tracheas. For the control tracheas, the percentage reduction in cross-sectional area varied between  $27 \pm 4\%$  at 20cm H<sub>2</sub>O and  $58 \pm 2\%$  at 80cm H<sub>2</sub>O. While collapse exceeded 50%, it only did so at pressures exceeding those of forced expiration and so this behavior would not be classified as malacic.

A single incision through the cartilage, however, was sufficient to produce airway reduction greater than 50% for pressures of 30cm H<sub>2</sub>O and higher. For a negative pressure peak of 80cm H<sub>2</sub>O, percentage CSA reduction just exceeds 70% indicating that a single incision provides a good model for mild TBM.

For 25% cartilage resection, lumen percentage CSA reduction exceeds 75% at 30cm H<sub>2</sub>O and exceeds 90% area reduction between 70 and 80cm H<sub>2</sub>O. Consequently, the 25% cartilage resection model corresponds to moderate TBM for most of the pressure range associated with forced exhalation.

In tracheas with 50% circumferential cartilage resection, the percentage collapse ranges from  $73 \pm 4\%$  to  $99 \pm 1\%$  as negative pressure was raised from 20cm to 80cm, respectively. This amount of resection produces a model of moderate TBM for pressures up to 40cm H<sub>2</sub>O and severe TBM at higher pressures.

One-way ANOVA tests performed for peak percentage collapse of the four experimental groups for each intratracheal pressure value showed significant difference ( $p < 1.3 \times 10^{-8}$ ).

***Stent testing enables tuning of design parameters***



Video 2 shows the real-time collapse of intratracheal lumens in unsupported and stent-supported iTBM trachea (CR50) under cyclic intratracheal peak pressure of 80cm of H<sub>2</sub>O. Figure 5 compares the collapse of the stented tracheas with 25% and 50% cartilage resection to that of the intact control tracheas. Comparing the stents with different pitches, corresponding to different unsupported lengths of tissue between the coils, it is observed that the stents with a 6mm pitch reduce airway collapse substantially more than what is observed in a control trachea (1-tail t-test:  $p < 0.008$ ). In contrast, the stent with a 12mm pitch produces an area reduction less than, but still close to that of the control trachea (2-tail t-test:  $p > 0.06$  for  $< 70$ cm H<sub>2</sub>O pressure). This suggests that the stents with a 6mm pitch are overly stiff.

In comparing Stents 2 and 3, which both have a 6mm pitch, Stent 2 uses the larger wire diameter and so is radially stiffer. The corresponding experimental result is that it experiences slightly less area reduction than Stent 3 (2-tail test-test:  $p > 0.05$ ). Taken together, these tests suggest that further design optimizations should consider smaller wire diameters with a helical pitch of ~12mm.

### ***Airway collapse morphologies in intact and iTBM tracheas***

As shown in Figure 6, three different morphologies of cross-sectional contraction were observed during testing. In the control trachea, most of the contraction, as expected, occurs in the posterior membrane of the trachea (Figure 6A). Though not malacic, the shape is like the crescent type of TBM. In tracheas with a single incision, a significant lateral component of contraction is observed which is comparable to the Saber-sheath type of TBM (Figure 6B). In malacic tracheas with 25-50% cartilage resection, collapse occurs in all directions (Figure 6C-D) mimicking the circumferential type of TBM. Video 3 shows the intratracheal lumens in real-time

from the four experimental tracheas under cyclic peak negative intratracheal pressure of 80cm of H<sub>2</sub>O.

## DISCUSSION

Our results demonstrate that ex vivo testing systems can provide a valuable approach for performing stent design optimization and for refining in vivo animal models. Designing the testing system to apply cyclic pressures provides several benefits. First, the observed temporal variation in tracheal cross-section can be more closely related to physiologic variation over the breathing cycle. Second, it provides a means to precondition the tissue prior to data collection. Third, it avoids the permanent airway collapse associated with maintained static loading that was observed during system development.

When applied to stent design, the testing system enables rapid comparison of design alternatives in which critical parameters are varied. In the examples considered here, helical stents with different wire diameters and helical pitches were considered. The system provided the means to compare the pressure-dependent airway collapse of stented malacic tracheas with that of intact control tracheas. In this way, stent designs can be tuned to provide sufficient support without being overly stiff, which can potentially increase granulation tissue or cause tissue erosion.<sup>8, 25</sup>

In addition to stent design, the ex vivo testing system provides a means of interpreting animal models for TBM. For example, using the TBM model in which a portion of each cartilage ring is removed (Figure 4), we were able to relate the severity of the TBM with the amount

removed. A single cartilage incision produced mild TBM (50-75% area reduction) for pressures associated with forced exhalation. Similarly, removing 25% of the cartilage rings produced moderate TBM (76-90% area reduction) while removing 50% of the rings produced moderate to severe TBM (>91% area reduction). Furthermore, the intact control tracheas exhibited mild TBM for negative intratracheal pressures of 70cm H<sub>2</sub>O and above. While these pressures exceed those typically associated with forced exhalation,<sup>30</sup> they are well below those of coughing and support the ongoing controversy of assuming 50% area reduction is indicative of TBM.<sup>4</sup>

The results of this study can also aid in refining the design of animal studies, for example cartilage resection model of TBM. One could design in vivo experiments in which a specific desired degree of TBM is achieved. Without this knowledge, the temptation is to remove a large amount of cartilage to ensure that TBM occurs. This typically results in such severe TBM that the animal cannot survive without significant airway support. Such a model precludes the inclusion of unstented controls, causes animal loss and suffering in the case of stent migration or malfunction and is not representative of the majority of TBM patients.

### ***Limitations***

As in existing animal models, our model relies on inducing TBM by creating airway-wall weakness through removal of cartilage segments. This weakened airway-wall does not necessarily match the biomechanical properties of TBM airways. Acquiring or creating such TBM tracheas remains a challenge.

This study focused on inducing TBM by weakening or injury to the anterior aspect of the tracheal walls which present only circumferential and saber-sheath TBM morphologies. Collapse of posterior tracheal aspects creates EDAC or crescent type TBM which are the most common

morphology presented in the clinic. We plan future studies to quantify posterior collapse by injury to posterior tracheal aspect.<sup>29</sup>

Since the testing system uses ex vivo tissue, the measured cross-sectional collapse will differ from what would be measured in vivo for the same transmural pressure. This will be due to changes in the mechanical properties of the tissue and due to the changes in boundary conditions associated with excising the trachea from the surrounding tissues. While it is anticipated that the ex vivo results will approximate those of in vivo testing, future studies are needed to compare ex vivo and in vivo testing results. Such comparisons will improve our ability to interpret ex vivo results, i.e., to understand if ex vivo testing tends to overestimate or underestimate airway cross-sectional area as a function of pressure.

The testing system was designed to apply oscillating pressures to approximate physiologic variations in airway cross-section during forced breathing while also enabling tissue preconditioning. To provide a more accurate representation of the respiratory cycle, the system could be enhanced to expand the pressure cycles that can be produced. In particular, to include inspiration, the system could be modified to vary pressure between a peak negative value and a peak positive value. A peak positive pressure of 10-20cm H<sub>2</sub>O would be sufficient.<sup>30</sup> Simulated coughing is also of interest, but this would likely require adding a separate cough generator as described by Freitag et al. to generate a rapid pressure pulse.<sup>21</sup>

## CONCLUSIONS

373           This study demonstrates how an ex vivo tracheal testing system can be used to interpret  
374 and refine TBM animal models. It also provides a cost-effective and time-efficient complement  
375 to mechanical and in vivo testing of stent prototypes.

## FIGURE LEGENDS

**Figure 1.** Ex vivo testing system. (A) Schematic showing major components. The linear actuator coupled with pneumatic cylinder (in dotted green box) creates and controls the intratracheal negative pressure. The trachea is placed over a warm water bath and sealed with pressure inlet on left end and endoscope camera on right (in dotted orange box). Based on commands from the PC, a microcontroller uses pressure measurements to control the actuator so as to produce the desired oscillatory pressure. (B) Testing system shown with an intact trachea.

**Figure 2.** Midanterior views of experimental tracheas. (A) Intact trachea. (B-E) Tracheas with induced TBM (iTBM) showing selected region for incision or resection spanning ~3cm. Different levels of TBM severity were induced by (B) single midanterior incision per cartilage, (C) 25% circumferential resection per cartilage and (D) 50% circumferential resection per cartilage. (E) An iTBM trachea (50% circumferentially resected cartilages) with an implanted helical stent.

**Figure 3.** Tracheal lumen contour detection and determination of percentage change in tracheal cross-sectional area. (A) Endoscopic view of tracheal lumen showing laser-lit contour in ambient light. (B) Endoscopic view of (A) in darkened room. The laser-lit contour is easily distinguishable. (C) Cropped and processed gray-scale image enhances the laser-lit tracheal-lumen contour (in white). (D) Plot showing intratracheal negative pressure and percentage collapse in tracheal cross-sectional area with time. Note time synchronization of plots is

approximate. (E) Automated tracheal lumen contour tracking (dotted green) using snake contour method at zero intratracheal pressure. (F) detected contour at negative 50cm H<sub>2</sub>O.

**Figure 4.** Percentage reduction in tracheal cross-section as a function of peak negative pressure. Ranges of area reduction associated with mild (51-75%), moderate (76-90%) and severe (>91%) are noted. The percentage collapse in the four experimental groups for each intratracheal pressure value had statistically significant differences (One-way ANOVA:  $p < 1.3 \times 10^{-8}$ ). EDAC - Excessive dynamic airway collapse.

**Figure 5.** Stent performance in treating moderate and severe iTBM. The percentage collapse in tracheal cross-sectional area vs intratracheal negative pressure plots in intact trachea (green) and iTBM tracheas treated with 3 helical stents of different pitch and wire diameters (ST1: P12mm, WD0.6mm, ST2: P6mm WD0.6mm and ST3: P6mm WD0.52mm). Each stent was tested in tracheas with 25% (lighter shade, CR25) and 50% (darker shade, CR50) cartilage removed. Plots indicate that 12mm pitch was sufficient to produce collapse close to that of an intact trachea (2-tail t-test:  $p > 0.06$  for <70cm H<sub>2</sub>O pressure). Stents with lower pitch (P6mm in ST2 and ST3) are overly stiff and reduce tracheal collapse significantly more than that of the control trachea (1-tail t-test:  $p < 0.01$ ). P - pitch, WD - wire diameter.

**Figure 6.** Tracheal collapse morphologies in control and different modes of iTBM. Dotted lines present the tracheal-lumen's profile at intratracheal negative pressure from 0 to 80cm H<sub>2</sub>O in (A) intact trachea, (B) trachea with single incision per cartilage, (C) trachea with 25% circumferential resection per cartilage and (D) trachea with 50% circumferential resection per

cartilage. Point or region of cartilage incision/resection are indicated using yellow arrows in the malacic tracheas (B-D). Direction(s) of collapse are indicated using blue arrows. In intact trachea the collapse occurs from posterior membranous tracheal wall (A) as expected during dynamic airway collapse. A single midanterior cartilage incision creates a hinge point, causing collapse to occur more laterally (B) as in the saber-sheath type TBM. Partial resection of cartilage rings causes the tracheal wall to collapse from all directions as in circumferential TBM.



**VIDEO LEGENDS**

**Video 1.** Intratracheal cross-sectional area calculation using automated video analysis in control trachea under cyclic peak negative intratracheal pressure of 50cm of H<sub>2</sub>O.

**Video 2.** Endoscopic videos of LASER-lit tracheal lumen in unsupported and stent-supported iTBM trachea under cyclic peak negative intratracheal pressure of 80cm of H<sub>2</sub>O.

**Video 3.** Endoscopic videos of LASER-lit tracheal lumen in control (CTR) and iTBM tracheas (CSI, CR25 and CR50) under cyclic peak negative intratracheal pressure of 80cm of H<sub>2</sub>O.

**TABLES****Table 1.** Stent specifications

Stent	Helix pitch	Wire diameter
ST1	12mm	0.52mm
ST2	6mm	0.52mm
ST3	6mm	0.6mm

## REFERENCES

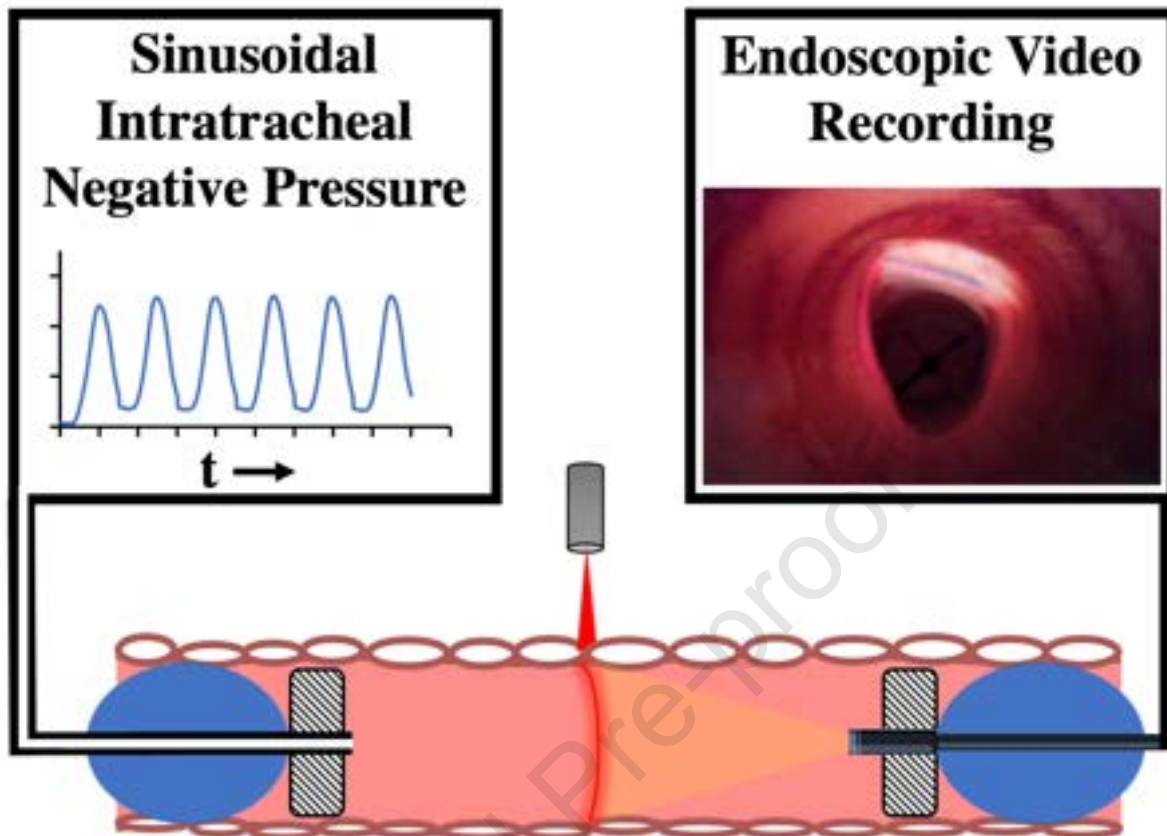
1. Ikeda S, Hanawa T, Konishi T, Adachi M, Sawai S, Chiba W, et al. Diagnosis, incidence, clinicopathology and surgical treatment of acquired tracheobronchomalacia. *Nihon Kyobu Shikkan Gakkai Zasshi*. 1992;30:1028-1035.
2. Carden KA, Boisselle PM, Waltz DA, Ernst A. Tracheomalacia and Tracheobronchomalacia in Children and Adults: An In-depth Review. *Chest*. 2005;127:984-1005.
3. Murgu S, Colt H. Tracheobronchomalacia and excessive dynamic airway collapse. *Clin Chest Med*. 2013;34:527-555.
4. Majid A, Gaurav K, Sanchez JM, Berger RL, Folch E, Fernandez-Bussy S, et al. Evaluation of tracheobronchomalacia by dynamic flexible bronchoscopy. A pilot study. *Ann Am Thorac Soc*. 2014;11:951-955.
5. Aslam A, Cardenas JDL, Morrison RJ, Lagisetty KH, Litmanovich D, Sella EC, et al. Tracheobronchomalacia and Excessive Dynamic Airway Collapse: Current Concepts and Future Directions. *RadioGraphics*. 2022;42:1012-1027.
6. Boisselle PM, O'Donnell CR, Bankier AA, Ernst A, Millet ME, Potemkin A, et al. Tracheal collapsibility in healthy volunteers during forced expiration: assessment with multidetector CT. *Radiology*. 2009;252:255-262.
7. Lazzaro RS, Bahrolloomi D, Wasserman GA, Patton BD. Robotic Tracheobronchoplasty: Technique. *Operative Techniques in Thoracic and Cardiovascular Surgery*. 2022;27:218-226.
8. Folch E, Keyes C. Airway stents. *Ann Cardiothorac Surg*. 2018;7:273-283.

- 467 **9.** Morrison RJ, Hollister SJ, Niedner MF, Mahani MG, Park AH, Mehta DK, et al.  
 468 Mitigation of tracheobronchomalacia with 3D-printed personalized medical devices in  
 469 pediatric patients. *Sci Transl Med.* 2015;7:285ra264.
- 470 **10.** Sztano B, Kiss G, Marai K, Racz G, Szegedi I, Racz K, et al. Biodegradable airway  
 471 stents in infants - Potential life-threatening pitfalls. *Int J Pediatr Otorhinolaryngol.*  
 472 2016;91:86-89.
- 473 **11.** Zopf DA, Flanagan CL, Wheeler M, Hollister SJ, Green GE. Treatment of severe porcine  
 474 tracheomalacia with a 3-dimensionally printed, bioresorbable, external airway splint.  
 475 *JAMA Otolaryngol Head Neck Surg.* 2014;140:66-71.
- 476 **12.** Dutau H, Musani AI, Laroumagne S, Darwiche K, Freitag L, Astoul P. Biodegradable  
 477 Airway Stents - Bench to Bedside: A Comprehensive Review. *Respiration.* 2015;90:512-  
 478 521.
- 479 **13.** Bolliger CT, Probst R, Tschopp K, Soler M, Perruchoud AP. Silicone stents in the  
 480 management of inoperable tracheobronchial stenoses. Indications and limitations. *Chest.*  
 481 1993;104:1653-1659.
- 482 **14.** FDA. Public Health Notification: Complications from Metallic Tracheal Stents in  
 483 Patients with Benign Airway Disorders 2005.
- 484 **15.** Sztano B, Rovo L. Response to the letter to the Editor "Biodegradable airway stents in  
 485 infants - Potential life-threatening pitfalls". *Int J Pediatr Otorhinolaryngol.* 2017;98:175-  
 486 176.
- 487 **16.** Vondrys D, Anton-Pacheco Sanchez J. Letter to the Editor regarding "Biodegradable  
 488 airway stents in infants - Potential life-threatening pitfalls". *Int J Pediatr*  
 489 *Otorhinolaryngol.* 2017;98:174.

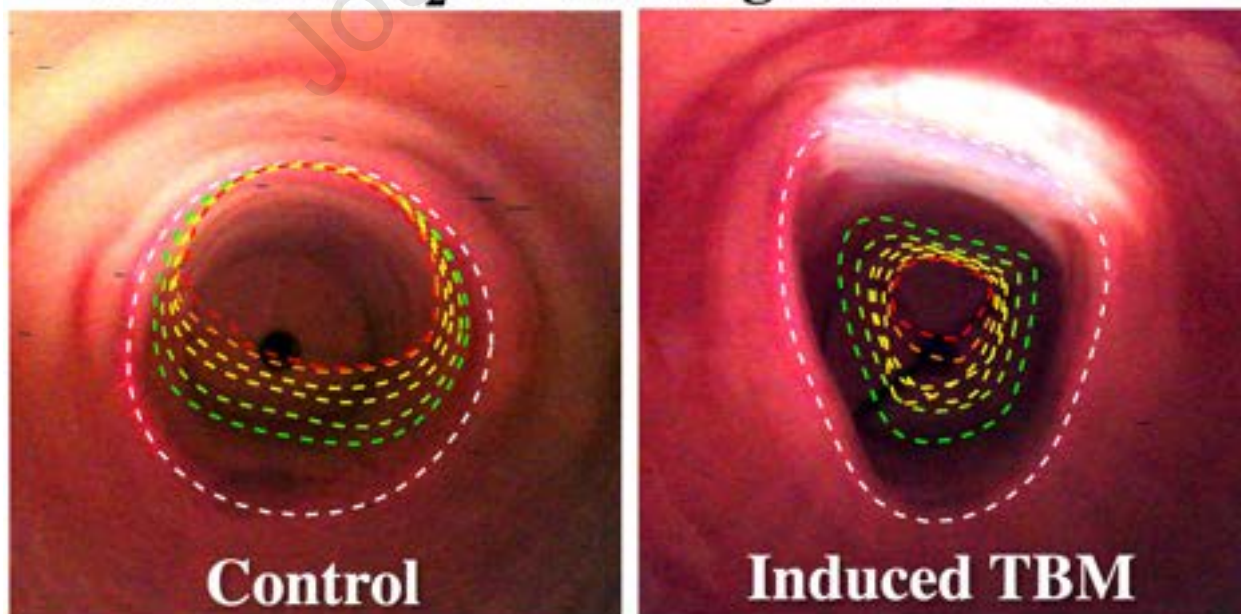
- 490 **17.** Mencattelli M, Mondal A, Miale R, Van Story D, Peine J, Li Y, et al. In Vivo Molding of  
491 Airway Stents. *Advanced Functional Materials*. 2021;31:2010525.
- 492 **18.** Mondal A, Ha J, Jo VY, Wu FY, Kaza AK, Dupont PE. Preclinical evaluation of a  
493 pediatric airway stent for tracheobronchomalacia. *J Thorac Cardiovasc Surg*.  
494 2020;161:e51-e60.
- 495 **19.** Ha J, Mondal A, Zhao Z, Kaza AK, Dupont PE. Pediatric Airway Stent Designed to  
496 Facilitate Mucus Transport and Atraumatic Removal. *IEEE Trans Biomed Eng*.  
497 2020;67:177-184.
- 498 **20.** Serrano-Casorran C, Lopez-Minguez S, Rodriguez-Zapater S, Bonastre C, Guirola JA,  
499 De Gregorio MA. A new airway spiral stent designed to maintain airway architecture  
500 with an atraumatic removal after full epithelization-Research of feasibility and viability  
501 in canine patients with tracheomalacia. *Pediatr Pulmonol*. 2020;55:1757-1764.
- 502 **21.** Freitag L, Eicker R, Linz B, Greschuchna D. Theoretical and experimental basis for the  
503 development of a dynamic airway stent. *European Respiratory Journal*. 1994;7:2038-  
504 2045.
- 505 **22.** Jung HS, Chae G, Kim JH, Park CY, Lim S, Park SE, et al. The mechanical  
506 characteristics and performance evaluation of a newly developed silicone airway stent  
507 (GINA stent). *Scientific Reports*. 2021;11.
- 508 **23.** Ryu YJ, Kim H, Yu CM, Choi JC, Kwon YS, Kim J, et al. Comparison of natural and  
509 Dumon airway stents for the management of benign tracheobronchial stenoses.  
510 *Respirology*. 2006;11:748-754.
- 511 **24.** Freitag L, Eicker K, Donovan TJ, Dimov D. Mechanical Properties of Airway Stents.  
512 *Journal of Bronchology & Interventional Pulmonology*. 1995;2:270-278.

- 513   **25.**   Hu HC, Liu YH, Wu YC, Hsieh MJ, Chao YK, Wu CY, et al. Granulation tissue  
514           formation following Dumon airway stenting: the influence of stent diameter. *Thorac*  
515           *Cardiovasc Surg.* 2011;59:163-168.
- 516   **26.**   Tsukada H, O'Donnell CR, Garland R, Herth F, Decamp M, Ernst A. A novel animal  
517           model for hyperdynamic airway collapse. *Chest.* 2010;138:1322-1326.
- 518   **27.**   Vinograd I, Filler RM, England SJ, Smith C, Poenaru D, Baboric A, et al.  
519           Tracheomalacia: An experimental animal model for a new surgical approach. *Journal of*  
520           *Surgical Research.* 1987;42:597-604.
- 521   **28.**   Kaye R, Goldstein T, Aronowitz D, Grande DA, Zeltsman D, Smith LP. Ex vivo  
522           tracheomalacia model with 3D-printed external tracheal splint. *Laryngoscope.*  
523           2017;127:950-955.
- 524   **29.**   Cao A, Swami P, Kaye R, Goldstein T, Grande DA, Smith LP. An Ex Vivo Model of  
525           Posterior Tracheomalacia With Evaluation of Potential Treatment Modalities.  
526           *Laryngoscope.* 2022.
- 527   **30.**   Loring SH, O'Donnell CR, Feller-Kopman DJ, Ernst A. Central Airway Mechanics and  
528           Flow Limitation in Acquired Tracheobronchomalacia. *CHEST.* 2007;131:1118-1124.
- 529   **31.**   Fung YC. *Biomechanics: Mechanical Properties of Living Tissues*: Springer New York;  
530           1981.
- 531   **32.**   Safshekan F, Tafazzoli-Shadpour M, Abdouss M, Shadmehr MB. Mechanical  
532           Characterization and Constitutive Modeling of Human Trachea: Age and Gender  
533           Dependency. *Materials (Basel).* 2016;9.

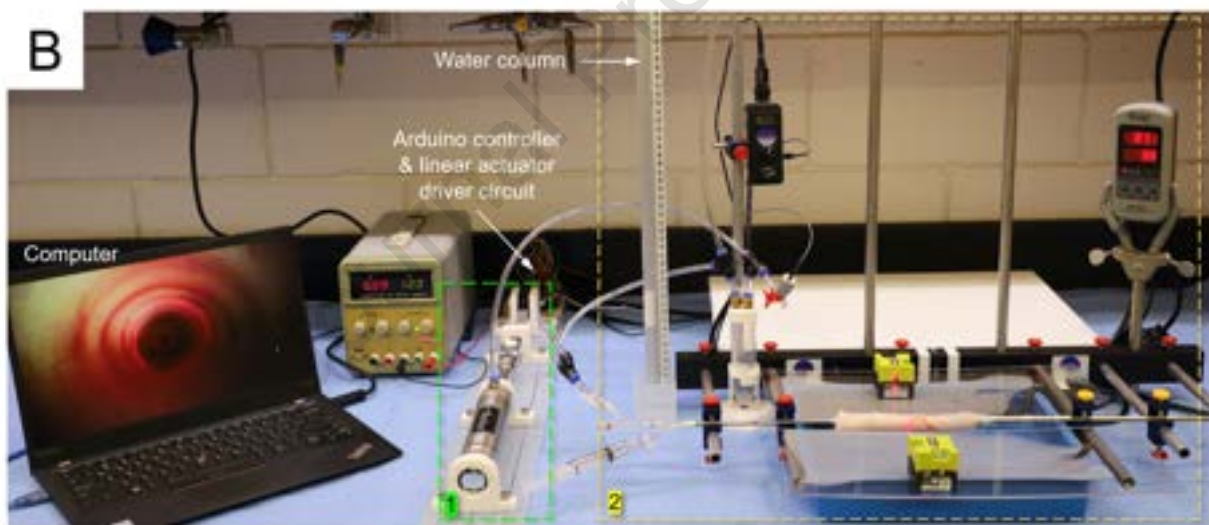
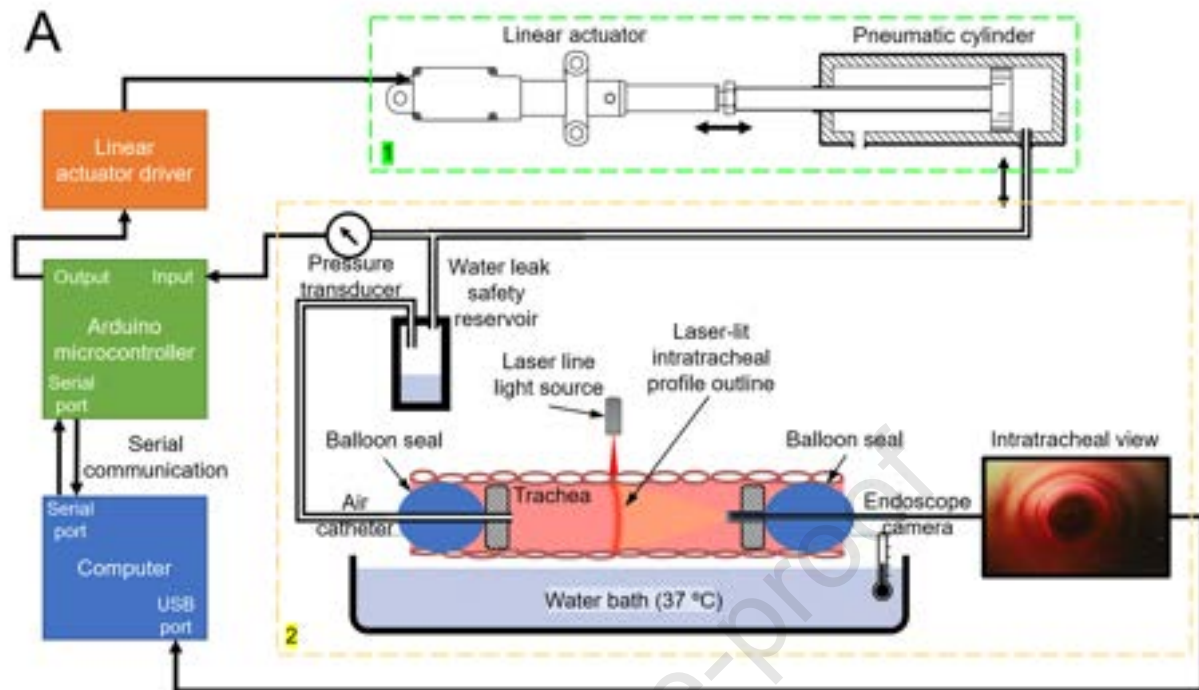
- 534 **33.** Bagnoli P, Acocella F, Di Giancamillo M, Fumero R, Costantino ML. Finite element  
535 analysis of the mechanical behavior of preterm lamb tracheal bifurcation during total  
536 liquid ventilation. *J Biomech.* 2013;46:462-469.
- 537 **34.** Kumar R. Snakes: Active Contour Models. MATLAB Central File Exchange.
- 538 **35.** Xu C, Prince JL. Snakes, shapes, and gradient vector flow. *IEEE Trans Image Process.*  
539 1998;7:359-369.
- 540

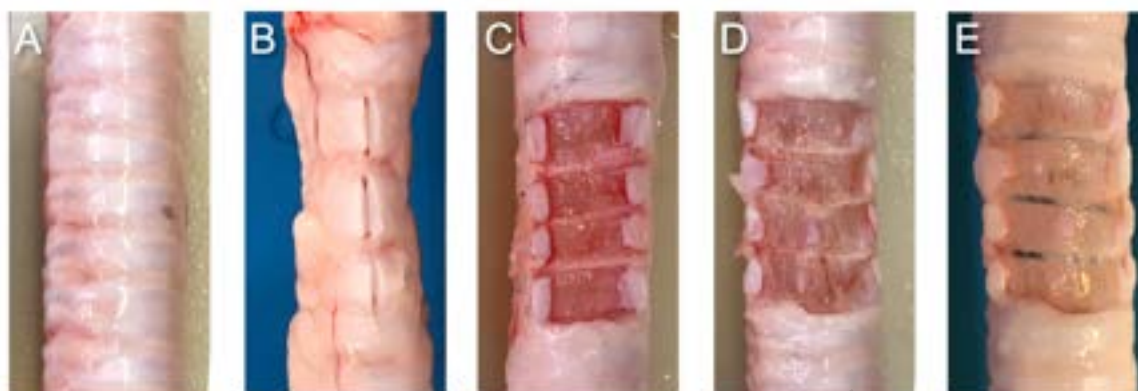


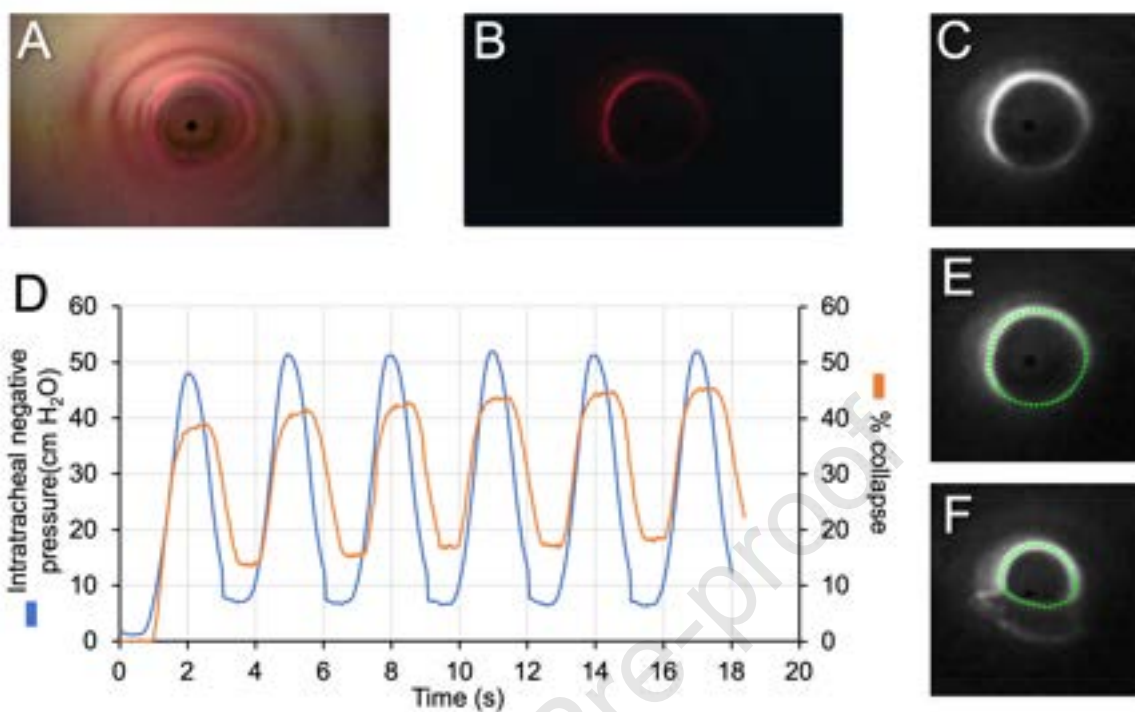
**Intratracheal Lumen Contours at  
0 to 80cm H<sub>2</sub>O Peak Negative Pressure**

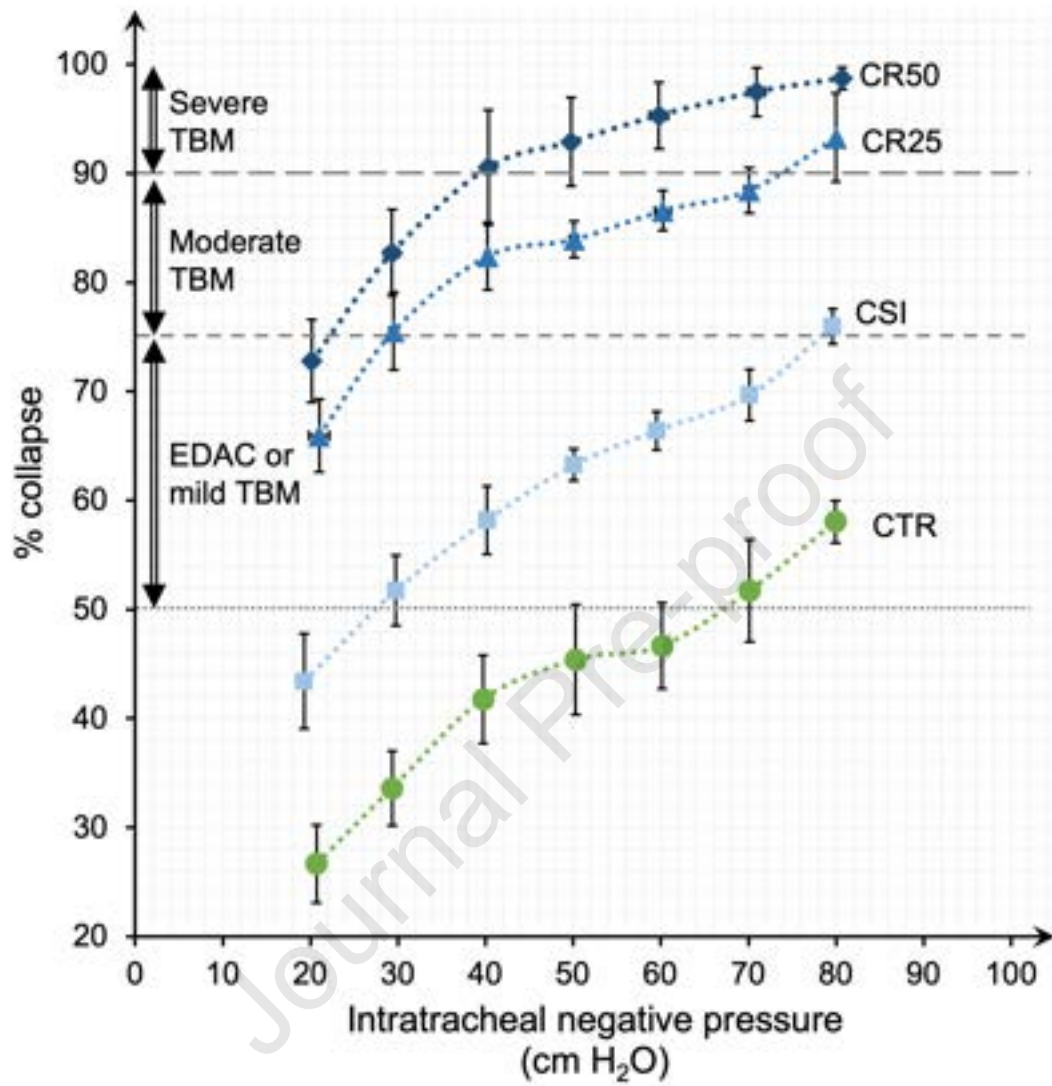


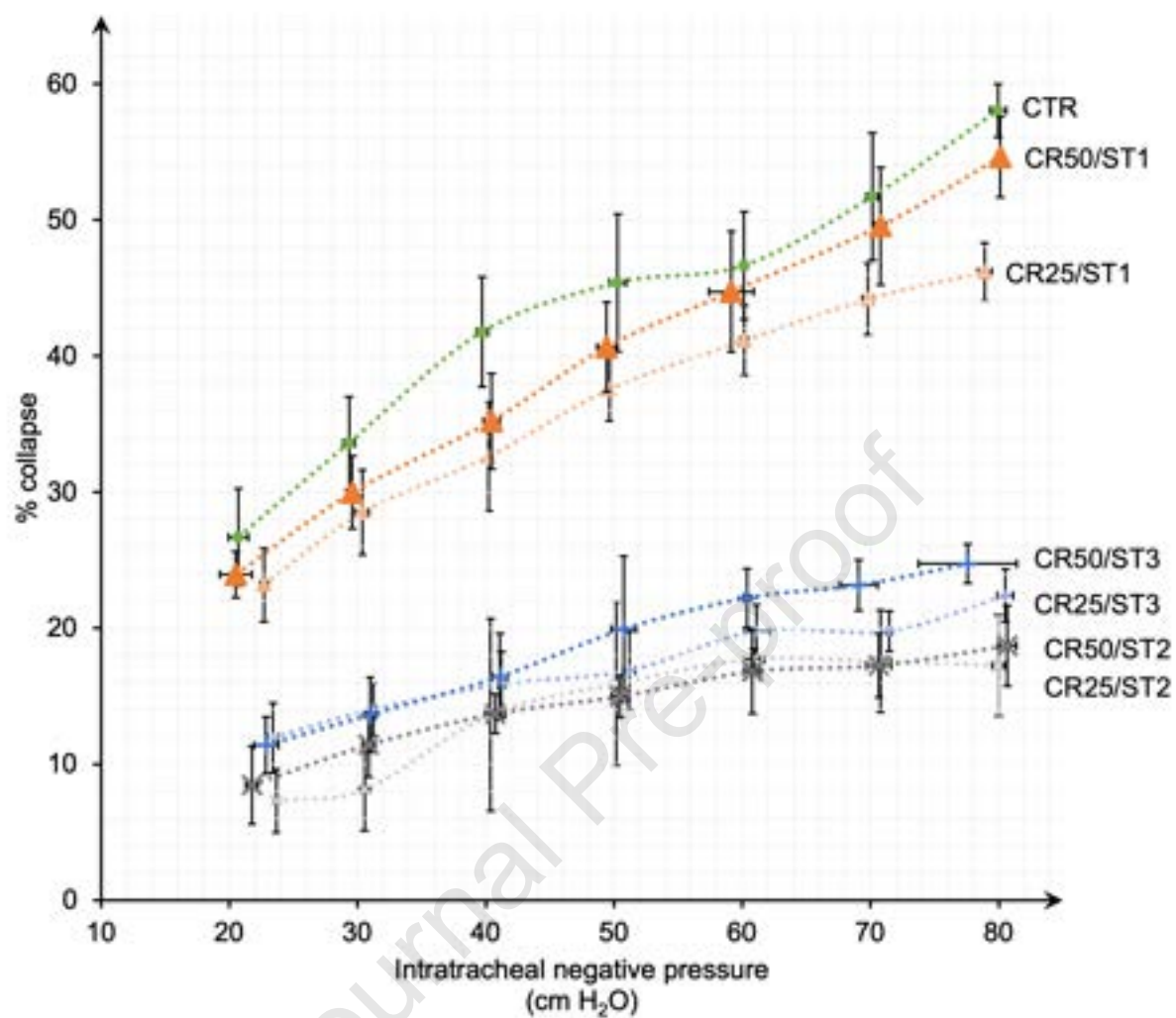


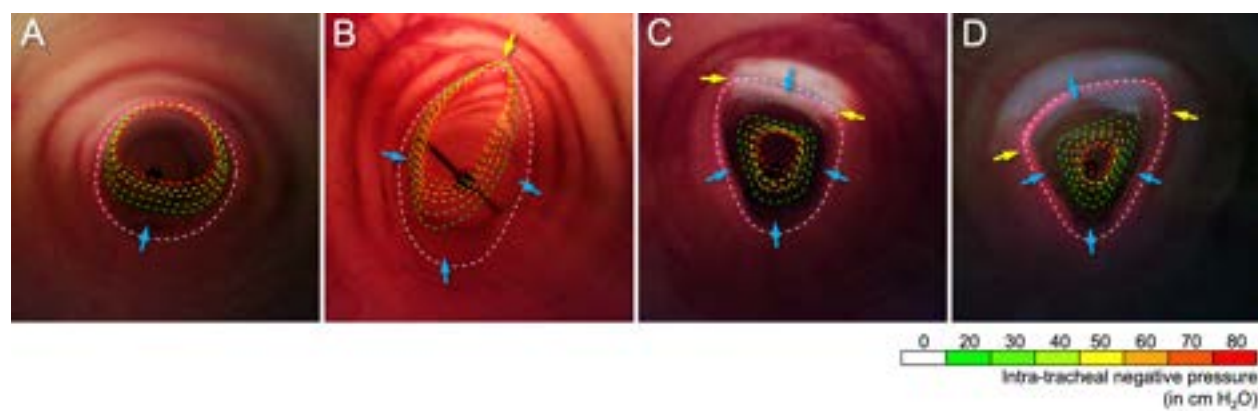












**Supplementary Table 1: Experimental conditions**

<b>S#</b>	<b>Group</b>	<b>Experimental condition</b>	<b>n</b>
1	CTR	Intact trachea (control)	4
2	CSI	Trachea with single incision per cartilage	4
3	CR25	Trachea with 25% radially resected cartilage	4
4	CR50	Trachea with 50% radially resected cartilage	4
5	CR25/ST1	25% cartilage resected trachea treated with stent 1	3
6	CR25/ST2	25% cartilage resected trachea treated with stent 2	3
7	CR25/ST3	25% cartilage resected trachea treated with stent 3	3
8	CR50/ST1	50% cartilage resected trachea treated with stent 1	3
9	CR50/ST2	50% cartilage resected trachea treated with stent 2	3
10	CR50/ST3	50% cartilage resected trachea treated with stent 3	3